



Structural Reorganization of the Third Metatarsal Bone Shaft After Autogenous Plasty of the Tibial Portion of the Sciatic Nerve

Nathalia A. Shchudlo, Tatyana A. Stupina, Tatyana N. Varsegova

National Ilizarov Medical Research Centre for Traumatology and Orthopedics, Kurgan, Russia

Abstract

Background. Previous research has shown that neurectomy of the sciatic nerve leads to a reduction in bone density in the femur and tibia of laboratory mice and rats. However, the impact of surgeries aimed at restoring nerve innervation on the bones of distal limb parts has not been studied.

Aim of the study – to identify structural changes in the shaft of the third metatarsal bone after primary autogenous plasty of the resection defect of the tibial portion of the sciatic nerve in rats.

Methods. Autologous neuroplasty of the tibial portion of the sciatic nerve was performed on 16 Wistar rats (aged 8–10 months). The animals were euthanized at 4 and 6 months after the surgery, and a control group of 7 intact rats of similar age was included. Histomorphometric analysis was conducted on a dissected fragment of the forefoot at the level of the metatarsal bones. The ratio of fuchsinophilic and anilinophilic structures of the cortical plate was determined using point-count volumetry on Masson-stained images of transverse sections of the third metatarsal bone shaft. The thickness of the cortical plate, numerical density, area, and diameter of osteons and Haversian canals were measured.

Results. After 4 months, compared to the control group, a 15% decrease ($p = 0.0001$) in the proportion of mineralized structures of the cortical plate and a 12.7% reduction ($p = 0.0184$) in its thickness were observed. Osteolysis signs were present in the osteonal layer, along with decreased numerical density and dimensional characteristics of osteons, and the presence of osteons with dilated Haversian canals. At 6 months, the thickness of the cortical plate did not significantly differ from the norm ($p = 0.2067$), but there was a progressive 33.6% decrease ($p = 0.0001$) in the proportion of mineralized structures. Reduced values of numerical density, area, and diameter of osteons persisted in the osteonal layer, while the diameters of Haversian canals in osteons increased over time.

Conclusion. From 4 to 6 months, the thickness of the cortical layer in the compact bone of the third metatarsal bone shaft was restored. However, changes in the numerical and dimensional composition of osteons, along with decreased mineralization of the extracellular matrix and erosion of the subperiosteal bone layer, continued to progress. The developed experimental 2D model can be used to assess denervation osteopenia in distal limb parts and further explore rehabilitation interventions that enhance and improve reinnervation.

Keywords: rat sciatic nerve, autoneuroplasty, metatarsal bone shaft, denervation osteopenia, histomorphometry.

Cite as: Shchudlo N.A., Stupina T.A., Varsegova T.N. Structural Reorganization of the Third Metatarsal Bone Shaft After Autogenous Plasty of the Tibial Portion of the Sciatic Nerve. *Traumatology and Orthopedics of Russia*. 2023;29(3):56–64. (In Russian).

✉ Tatyana A. Stupina; e-mail: stupinasta@mail.ru

Submitted: 26.01.2023. Accepted: 15.06.2023. Published online: 11.07.2023

© Shchudlo N.A., Stupina T.A., Varsegova T.N., 2023



Структурная реорганизация диафиза III плюсневой кости после аутогенной пластики большеберцовой порции седалищного нерва

Н.А. Щудло, Т.А. Ступина, Т.Н. Варсегова

ФГБУ «Национальный медицинский исследовательский центр травматологии и ортопедии им. акад. Г.А. Илизарова» Минздрава России, г. Курган, Россия

Реферат

Введение. Из мировой литературы известно влияние нейрэктомии седалищного нерва на снижение костной плотности бедренных и большеберцовых костей лабораторных мышей и крыс, но не изучено состояние костей дистальных отделов конечностей после операций, направленных на восстановление иннервации.

Цель исследования — выявить структурные изменения диафиза III плюсневой кости после первичной аутогенной пластики резекционного дефекта большеберцовой порции седалищного нерва крыс.

Материал и методы. У 16 крыс Wistar (возраст 8–10 мес.) выполнена аутологичная нейропластика большеберцовой порции седалищного нерва. Через 4 мес. ($n = 8$) и 6 мес. ($n = 8$) после операции животных эвтаназировали. Группу контроля (контроль) составили 7 интактных животных в возрасте 14 мес. ($n = 3$) и 16 мес. ($n = 4$) — соответственно возрасту оперированных крыс на момент эвтаназии. Для гистоморфометрического анализа иссекали фрагмент переднего отдела стопы на уровне плюсневых костей. Методом точко-счетной объемометрии в изображениях поперечных срезов диафиза III плюсневой кости, окрашенных по Массону, определяли соотношение фуксинофильных и анилинофильных структур кортикальной пластинки. Измеряли толщину кортикальной пластинки, определяли численную плотность, площадь и диаметр остеонов и гаверсовых каналов.

Результаты. Через 4 мес. эксперимента по сравнению с контролем выявлено снижение доли минерализованных структур кортикальной пластинки на 15% ($p = 0,0001$), уменьшена ее толщина на 12,7% ($p = 0,0184$). В остеонном слое выражены признаки остеолита, снижена численная плотность остеонов, их размерные характеристики, отмечены остеоны с расширенными гаверсовыми каналами. В срок 6 мес. толщина кортикальной пластинки не имела статистически значимых отличий от нормы ($p = 0,2067$), однако прогрессировало снижение доли минерализованных структур — на 33,6% ($p = 0,0001$). В остеонном слое сохранялись сниженные значения численной плотности остеонов, их площади и диаметров. Значения диаметров гаверсовых каналов остеонов продолжали увеличиваться.

Заключение. В период от 4 до 6 мес. восстанавливалась толщина кортикальной пластинки диафиза III плюсневой кости, но прогрессировали изменения численно-размерного состава остеонов, уменьшение минерализации внеклеточного матрикса и эрозирование субпериостального слоя кости. Оценка денервационной остеопении дистальных отделов конечностей в данных условиях эксперимента применима в дальнейших исследованиях реабилитационных воздействий, ускоряющих и улучшающих реиннервацию.

Ключевые слова: седалищный нерв крысы, аутонейропластика, диафиз плюсневой кости, денервационная остеопения, гистоморфометрия.

Для цитирования: Щудло Н.А., Ступина Т.А., Варсегова Т.Н. Структурная реорганизация диафиза III плюсневой кости после аутогенной пластики большеберцовой порции седалищного нерва. *Травматология и ортопедия России*. 2023;29(3):56-64.

Ступина Татьяна Анатольевна; e-mail: stupinasta@mail.ru

Рукопись получена: 26.01.2023. Рукопись одобрена: 15.06.2023. Статья опубликована онлайн: 11.07.2023

© Щудло Н.А., Ступина Т.А., Варсегова Т.Н., 2023

BACKGROUND

The study of bone structure changes in peripheral nerve injuries has been ongoing for many years. According to J.A. Gillespie, these changes are a result of muscular atrophy due to inactivity, and there is no evidence of specific trophic effects of nerves on bones [1]. However, as early as the first half of the 20th century, vasomotor nerves of Haversian canals and nerve fibers in the bone matrix were discovered [2]. In the last two decades, research on bone innervation has intensified [3], demonstrating the involvement of peripheral nerves in bone development and repair through neurotransmitters, neuropeptides, axonal growth factors, and neurotrophins [4]. Neural regulation of osteoblast and osteoclast function in both normal and pathological conditions, particularly osteoporosis, has been studied [5, 6, 7]. It has been established that the pathogenesis of "spot" osteoporosis in post-traumatic complex regional pain syndrome (CRPS), previously known as "reflex sympathetic dystrophy" or "causalgia" (in patients with peripheral nerve injuries), involves not only the peripheral but also the central nervous system [8]. Radiologically, spotted osteoporosis is often detected in the wrists and feet, predominantly affecting the subchondral bone. According to some authors, it does not lead to fractures and resolves spontaneously in most cases [9]. However, other specialists argue that the development of therapy aimed at increasing bone density is necessary for such patients [10].

Animal studies have shown a systemic decrease in bone density with chronic constriction of the sciatic nerve [11, 12] and after neurectomy [13, 14]. Separation, anisotropy, disruption of continuity, and reduced trabecular density in the proximal metaphysis of the tibia were more pronounced after sciatic neurectomy than in ovariectomized rats [13]. On the other hand, bone loss in ovariectomized rats was also associated with decreased intracortical innervation [15].

Bone density loss after sciatic neurectomy occurs more intensively in trabecular bone than in compact bone [16]. However, in the cortical plate of the mouse tibia, accelerated bone resorption and decreased bone formation rate were observed as early as 4 weeks after sciatic neurectomy [13]. A similar result was obtained in rats, with a decrease in bone density occurring in a distal-proximal direction [17].

Pharmacological suppression of macrophages [18], low-intensity loading [19], low-frequency electric myostimulation [20], and the use of the flavonoid naringenin [21] have been shown to slow down bone mass loss induced by neurectomy.

However, the available literature does not provide information on changes in the microstructure of bones in the distal parts of the limbs after nerve surgeries aimed at restoring limb innervation.

The aim of the study was to identify structural changes in the diaphysis of the third metatarsal bone after primary autogenous plasty of the resection defect of the tibial portion of the sciatic nerve in rats.

METHODS

The study was conducted on 23 male Wistar rats aged 8-10 months with a body weight of 360-420 g. Autologous neuroplasty of the tibial portion of the sciatic nerve at the mid-third of the thigh was performed on 16 experimental animals, as described in our previously published article [22] (Fig. 1). At 4 and 6 months after the surgery, the animals were euthanized with an overdose of thiopental after premedication: Rompun 2% (1-2 mg/kg) and Zoletil 100 (10-15 mg/kg). The control group consisted of 7 intact animals aged 14-16 months, corresponding to the age of the operated rats at the time of euthanasia.

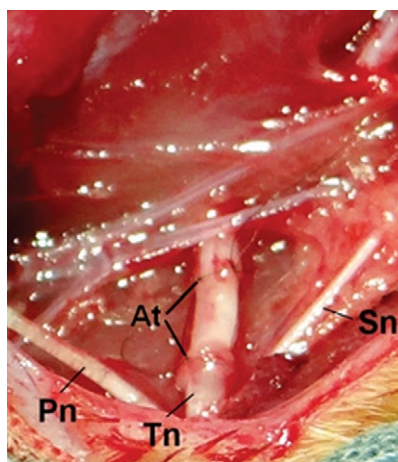


Fig. 1. Tibial portion (Tn) of the sciatic nerve after suturing the autologous graft (At) with 10-0 thread, Pn — peroneal portion of the sciatic nerve, Sn — sural nerve

For histomorphometric analysis, a fragment of the anterior part of the foot at the level of the metatarsal bones was dissected. The specimens were fixed in 10% formalin solution, partially decalcified in a mixture of hydrochloric and formic acid (needle test), dehydrated in ethanol, and embedded in paraffin. Paraffin sections (thickness: 5-7 μm) were prepared using an NM 450 Thermo Scientific microtome (USA), stained with hematoxylin and eosin, and with the trichrome method according to Masson. Light microscopy, digitization, and morphometry were performed using an AxioScope.A1 microscope with an AxioCam digital camera and Zenblue software (Carl Zeiss MicroImaging GmbH, Germany). The object of histomorphometric analysis was the diaphysis of the third metatarsal bone innervated by branches of the tibial nerve.

Using the point-count volumetry method in full-color digital images of transverse sections of the bone diaphysis stained with Masson's trichrome, the percentage (%) of fuchsinophilic (red-stained) and anilinophilic (blue-stained) structures of the cortical plate was determined. The measurements were performed at 400x magnification using the PhotoFiltre 7 program with a test grid of equidistant points with transparent centers [23]. Morphometry was conducted using the Zenblue software (Carl Zeiss MicroImaging GmbH, Germany) with the following parameters: at 40x magnification, the thickness of the cortical plate (h , μm) was measured, and at 400x magni-

fication, the numerical density of osteons (N_a), area of osteons (S , μm^2), diameter of osteons (d , μm), and diameter of Haversian canals (d_c , μm) were determined. 10 to 15 fields of view were analyzed for each case.

Statistical analysis

Data analysis was performed using descriptive statistics. Quantitative characteristics are presented as medians and quartiles (Me, Q1-Q3). Non-parametric Wilcoxon test was used to test statistical hypotheses for differences, and differences were considered statistically significant at $p < 0.05$ (AtteStat software, version 9.3.1).

RESULTS

In the intact group of animals, the cortical plate of the third metatarsal bone exhibited well-defined outer and inner layers of the general plates, with the osteonal layer located between them (Fig. 2a). The osteonal layer showed structurally mature osteons with narrow Haversian canal lumens.

In the experimental group, a similar structure was observed, but there were osteons with dilated Haversian canals (resorptive-type osteons), indicating bone loss due to resorption of compact bone substance around blood vessels (Fig. 2b). The Haversian canals were dilated and filled with erythrocytes. Changes in the extracellular matrix, such as the disruption of clear boundaries of osteons and the architecture of bone plates, were observed.

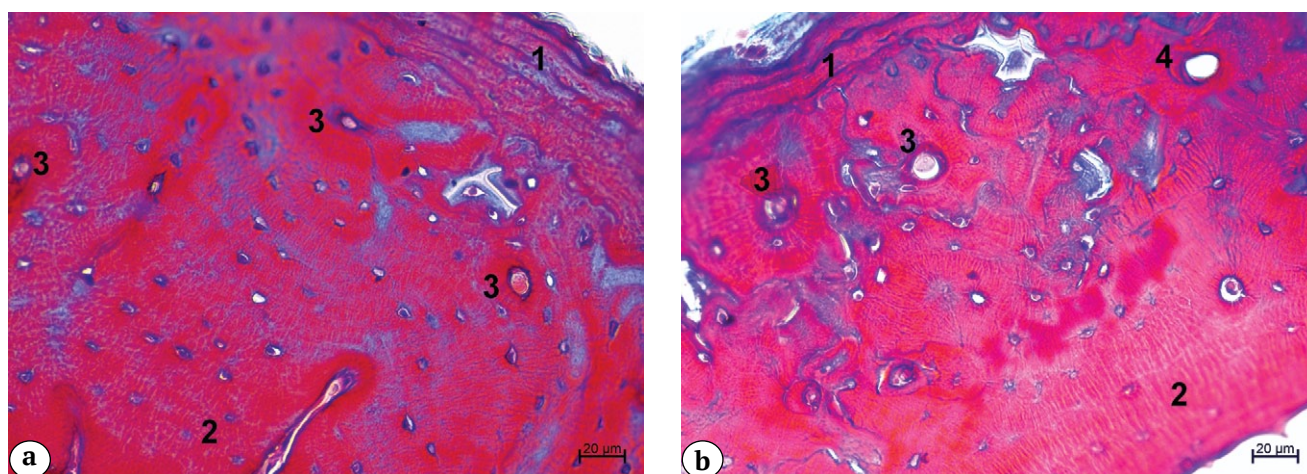


Fig. 2. Fragments of the cortical plate of the third metatarsal bone. Experimental period — 4 months: a — control (intact animals); b — experimental group; 1 — outer layer of the cortical plates; 2 — inner layer of the cortical plates; 3 — mature osteon; 4 — resorptive-type osteon. Cross-section; stained using the Masson's trichrome method. Mag. $\times 400$

At 4 months of the experiment, a decrease in the intensity of red staining in the sections of the cortical plate, particularly in the osteonal layer, was noted compared to the control group. The percentage of fuchsinophilic structures was reduced by 15% compared to the control (Table 1). The frequency of occurrence of osteoclasts was 0-2 per field of view at 400x magnification.

At 6 months of the experiment, visually increased proportions of anilinophilic structures were observed in the Masson's trichrome-stained

sections (Fig. 3). Quantitative analysis revealed a 33.6% decrease in the percentage of fuchsinophilic structures relative to the control (Table 1), indicating progressive reduction in cortical plate mineralization. Signs of periosteal resorption of the cortical plate were detected, and ingrowth of blood vessels and active osteoclasts were observed from the surrounding soft tissues (Fig. 3).

The outer layer of the general plates was thin in most observations, with some areas showing thickening. The osteonal layer exhibited signs of osteolysis, with reduced size of osteons and ex-

Table 1

Ratio of mineralized and non-mineralized structures in the cortical plate during the experimental stages, Me (Q1–Q3)

Parameter	Mineralized structures (%)	Non-mineralized structures (%)
Control	77.28 (74.93–79.06)	22.71 (19.89–24.51)
<i>4 months experiment</i>		
Experiment	65.33 (64.51–68.48)	34.66 (31.52–34.56)
p	$p^{k-o} = 0.0001$	$p^{k-o} = 0.0001$
<i>6 months experiment</i>		
Experiment	51.25 (46.25–58.66)	48.75 (41.33–51.33)
p	$p^{k-o} = 0.0001$; $p^{4-6} = 0.0018$	$p^{k-o} = 0.0001$; $p^{4-6} = 0.0018$

Wilcoxon test was used, and differences were considered statistically significant at $p < 0.05$; p^{k-o} - comparison between control and experimental groups; p^{4-6} - comparison between experiment durations.

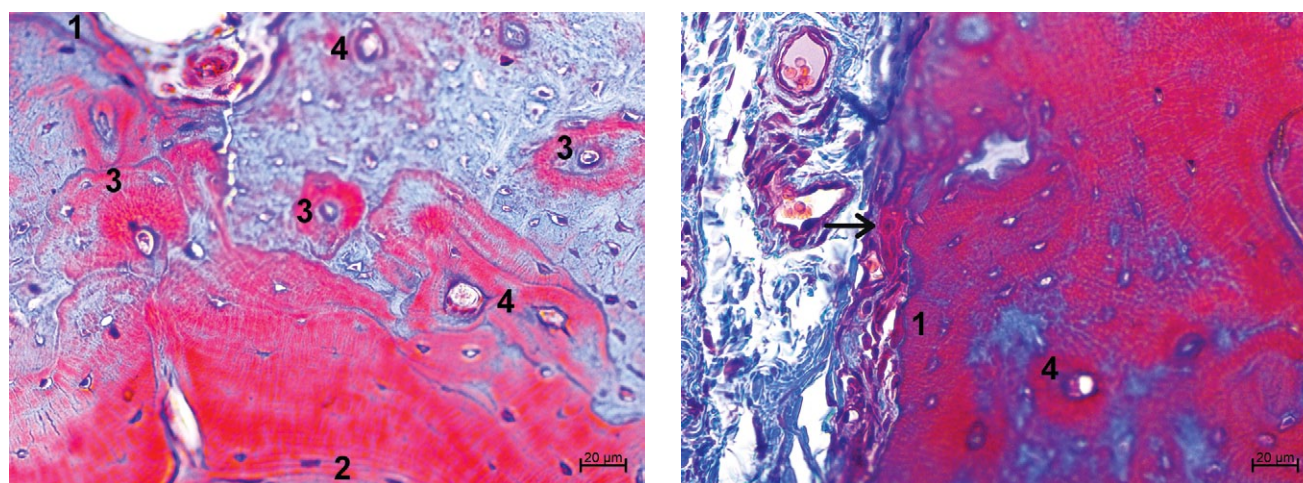


Fig. 3. Fragments of the cortical plate of the third metatarsal bone. Experimental period – 6 months: 1 – vascular invasion and osteoclast (arrow) in the outer layer of the bone plates; 2 – inner layer of the cortical plates; 3 – mature osteon; 4 – resorptive-type osteon. Cross-section; stained using the Masson's trichrome method. Mag. $\times 400$

panded Haversian canals with irregular contours (Fig. 3). The intensity of the resorption process was indicated by an increase in the frequency of occurrence of osteoclasts from 2 to 5 per field of view at 400x magnification.

In the histomorphometric analysis, the thickness of the cortical plate was significantly decreased in the experimental group compared to the control at 4 months of the experiment ($p = 0.0184$), but at 6 months, there were no significant differences compared to the intact group ($p = 0.2067$).

Throughout the experiment, the osteonal layer showed a decrease in the area and diameter of osteons compared to the control, with the lowest values observed at 4 months. The numerical density of osteons also progressively decreased. There was a statistically significant increase in the diameter of Haversian canals compared to the control ($p = 0.002$), and by the end of the experiment, the values of this parameter continued to increase (Table 2).

Table 2

Quantitative characteristics of the third metatarsal bone, Me (Q1–Q3)

Parameter	h cortical plate, μm	Na osteons	S osteon, μm^2	d osteon, μm	d haversian canal, μm
Control	332.39 (239.2/466.8)	5 (4/6)	1439.36 (629.69/1934.58)	37.48 (21.71/59.63)	5.63 (3.94/11.84)
<i>4 months experiment</i>					
Experiment	289.91 (260.17/302.26)	3.5 (3/4)	613.31 (435.06/954.82)	24.96 (21.14/56.59)	8.83 (7.47/15.26)
p	$p^{k-o} = 0.0184$	$p^{k-o} = 0.017$	$p^{k-o} = 0.008$	$p^{k-o} = 0.0085$	$p^{k-o} = 0.002$
<i>6 months experiment</i>					
Experiment	301.65 (256.80/327.03)	3 (2/3)	680.41 (311.07/987.07)	29.43 (19.18/45.65)	10.88 (7.64/25.29)
p	$p^{k-o} = 0.2067$ $p^{4-6} = 0.2701$	$p^{k-o} = 0.013$ $p^{4-6} = 0.0781$	$p^{k-o} = 0.0357$ $p^{4-6} = 0.9149$	$p^{k-o} = 0.0357$ $p^{4-6} = 0.5934$	$p^{k-o} = 0.0027$ $p^{4-6} = 0.3735$

Wilcoxon test was used, and differences were considered statistically significant at $p < 0.05$; p^{k-o} — comparison between control and experimental groups; p^{4-6} — comparison between experiment durations.

DISCUSSION

The primary end-to-end suture is considered the gold standard for surgical treatment of anatomical nerve injuries. However, complete functional recovery is achieved in only 10% of cases, as reported in a review of publications from 25 countries [24]. The main reasons for unsatisfactory clinical outcomes are believed to be the slow regenerative growth of axotomized neurons, which regenerates at a rate of only one inch per month in humans [25], and the long regenerative path, which predisposes to irreversible denervation changes in the target tissues of the distal extremities even before reinnervation occurs [26]. In particular, the degree of muscle changes can vary widely, reflecting the heterogeneity of the initial parameters of nerve injury and the different rates of atrophic compensatory processes. However, in the long term, the extent of these changes often becomes significantly pronounced [27].

However, not only in clinical practice but also in experiments on small laboratory animals, nerve regeneration parameters are restored slowly and partially. For example, up to 20 weeks after transection and suture of the sciatic nerve in rats, the ratio of peptidergic to non-peptidergic nerve fibers in the epidermis of foot pads remains disrupted [28]. According to other authors, 220 days after the sciatic nerve suture in rats, the average diameter of regenerating myelinated fibers in the distal nerve segment reaches no more than 50% of the corresponding parameter in the intact nerve, and the regenerating nerve contains a large number of thin non-conducting fibers [29].

In our previous experimental model of primary autoplasty of the resection defect of the sciatic nerve with a short autologous transplant, it was found that at 6 months after the surgery, the average diameter of regenerating myelinated fibers of the sciatic nerve at the middle third of the leg

was 52% of the corresponding parameter in the intact nerve. The vascularity index of the interosseous muscles of the sole was halved compared to intact animals, and the median diameter of muscle fibers was reduced by 20.96%, indicating partial reinnervation and reduced muscle vascularity in the foot [22].

In the present study, structural changes in the diaphysis of the third metatarsal bone were investigated for the first time in the long term after primary autoplasty of the sciatic nerve. In addition to the traditional hematoxylin and eosin staining for osteoporosis assessment [30], the Masson's trichrome staining method was used, which allows differentiation between mature mineralized bone and demineralized bone. The former exhibits an affinity for acidic fuchsin and is therefore stained red [31].

At 4 months of the experiment, a 15% decrease in the proportion of mineralized structures in the cortical plate compared to the control was found, and its thickness was reduced by 12.7%. The osteonal layer exhibited signs of osteolysis, decreased numerical density of osteons, and altered dimensional characteristics of osteons, including the presence of osteons with dilated Haversian canals. At 6 months, the thickness of the cortical plate did not show significant differences from the normal value, but there was a progressive decrease in the proportion of mineralized structures by 33.6%. Reduced numerical density, area, and diameter of osteons were observed in the osteonal layer. The diameters of Haversian canals of osteons increased over the course of the observation. The dilated Haversian canals with irregular contours were a result of osteoclastic resorption of bone tissue. By the end of the experiment, pronounced signs of periosteal resorption of the cortical plate were observed, and invasion of blood vessels and osteoclasts was registered from the surrounding soft tissues.

The dynamics of morphometric parameters of compact bone are likely determined by persistent reduction in vascularity of the surrounding soft tissues and the bone itself under conditions of incomplete reinnervation. The progressive increase in the diameter of Haversian canals and the restoration of cortical plate thickness may be related, as the formation of resorptive-type osteons provides a substrate for mineralization of the newly forming matrix.

It is also worth noting that the changes observed in our study are significantly different from disuse-related osteoporosis, which is characterized by a significant reduction in cortical plate thickness predominantly due to endosteal resorption [32], as well as from age-related osteopenia in rats, which is characterized by an increase in the numerical density of osteons and a decrease in the diameter of Haversian canals [33]. The development of age-related osteopenia in mice and humans is also manifested by an increase in cortical plate porosity due to the formation of osteon-like structures [34]. Biomechanical studies have shown that increased bone porosity leads to irreversible changes in shape through layer-by-layer compaction and destruction of the microstructure without fragmentation [35].

CONCLUSION

The results of the conducted study indicate that during the period of 4 to 6 months after autologous grafting of the resection defect of the tibial portion of the sciatic nerve, the thickness of the cortical plate of the diaphysis of the third metatarsal bone is restored. However, progressive changes in the numerical and dimensional composition of the osteons, decreased mineralization of the extracellular matrix, and erosion of the subperiosteal layer of the bone are observed. The developed experimental 2D model for evaluating denervation osteopenia in the distal parts of the limbs is applicable for further research on rehabilitation interventions that accelerate and improve reinnervation.

DISCLAIMERS

Author contribution

Shchudlo N.A. — study concept and design, writing and drafting the article.

Stupina T.A. — data analysis and interpretation, writing and drafting the article.

Varsegova T.N. — data analysis and interpretation, writing and drafting the article.

All authors have read and approved the final version of the manuscript of the article. All authors agree to bear responsibility for all aspects of the study to ensure proper consideration and resolution of all possible issues related to the correctness and reliability of any part of the work.

Funding source. State budgetary funding.

Disclosure competing interests. The authors declare that they have no competing interests.

Ethics approval. The study was conducted in compliance with the principles of humane treatment of laboratory animals in accordance with the requirements of the European Convention for the Protection of Vertebrate Animals used for Experiments and other Scientific Purposes and Directive 2010/63/EU of the European Parliament and the Council of the European Union of September 22, 2010 on the protection of animals used for scientific purposes.

The study was approved by the local ethics committee of National Ilizarov Medical Research Centre for Traumatology and Orthopedics, protocol No 4 (68), 11.11.2020.

Consent for publication. Not required.

REFERENCES

- Gillespie J.A. The nature of the bone changes associated with nerve injuries and disuse. *Bone Joint Surg.* 1954; 36-B(3):464-473. doi: 10.1302/0301-620X.36B3.464.
- Hurrell D.J. The Nerve Supply of Bone. *J Anat.* 1937; 72(Pt 1):54-61.
- Milovanović P., Đurić M. Innervation of bones: Why it should not be neglected? *Med Podml.* 2018;69(3):25-32. (In Serbian). doi: 10.5937/mp69-18404.
- Wan Q.Q., Qin W.P., Ma Y.X., Shen M.J., Li J., Zhang Z.B. et al. Crosstalk between Bone and Nerves within Bone. *Adv Sci (Weinh).* 2021;10;8(7):2003390. doi: 10.1002/advs.202003390.
- Gkiatas I., Papadopoulos D., Pakos E.E., Kostas-Agnantis I., Gelalis I., Vekris M. et al. The Multifactorial Role of Peripheral Nervous System in Bone Growth. *Front Phys.* 2017;5:44. doi: 10.3389/fphy.2017.00044.
- Tanashyan M.M., Antonova K.V., Mazur A.S., Spryshkov N.E. Neurological Diseases and Osteoporosis. *Effective pharmacotherapy.* 2022;18(19):42-50. (In Russian). doi: 10.33978/2307-3586-2022-18-19-42-50.
- Elefteriou F. Impact of the Autonomic Nervous System on the Skeleton. *Physiol Rev.* 2018;98(3):1083-1112. doi: 10.1152/physrev.00014.2017.
- Park G.Y., Im S., Hoon S. Patchy Osteoporosis in Complex Regional Pain Syndrome. *Osteoporosis. InTech;* 2012. Available from: <http://dx.doi.org/10.5772/29181>.
- Atkins R.M. Complex regional pain syndrome. *J Bone Joint Surg Br.* 2003;85(8):1100-1106. doi: 10.1302/0301-620x.85b8.14673.
- Hind K., Johnson M.I. Complex regional pain syndrome in a competitive athlete and regional osteoporosis assessed by dual-energy X-ray absorptiometry: a case report. *J Med Case Rep.* 2014;8:165. doi: 10.1186/1752-1947-8-165.
- Suyama H., Moriwaki K., Niida S., Maehara Y., Kawamoto M., Yuge O. Osteoporosis following chronic constriction injury of sciatic nerve in rats. *J Bone Miner Metab.* 2002;20(2):91-97. doi: 10.1007/s007740200012.
- Bosco F., Guarnieri L., Nucera S., Scicchitano M., Ruga S., Cardamone A. et al. Pathophysiological Aspects of Muscle Atrophy and Osteopenia Induced by Chronic Constriction Injury (CCI) of the Sciatic Nerve in Rats. *Int J Mol Sci.* 2023;24(4):3765. doi: 10.3390/ijms24043765.
- Brouwers J.E., Lambers F.M., van Rietbergen B., Ito K., Huiskes R. Comparison of bone loss induced by ovariectomy and neurectomy in rats analyzed by in vivo micro-CT. *J Orthop Res.* 2009;27(11):1521-1527. doi: 10.1002/jor.20913.
- Kodama Y., Dimai H.P., Wergedal J., Sheng M., Malpe R., Kutilek S. et al. Cortical tibial bone volume in two strains of mice: effects of sciatic neurectomy and genetic regulation of bone response to mechanical loading. *Bone.* 1999;25(2):183-190. doi: 10.1016/s8756-3282(99)00155-6.
- Burt-Pichat B., Lafage-Proust M.H., Duboeuf F., Laroche N., Itzstein C., Vico L. et al. Dramatic decrease of innervation density in bone after ovariectomy. *Endocrinology.* 2005;146(1):503-510. doi: 10.1210/en.2004-0884.
- Monzem S., Javaheri B., de Souza R.L., Pitsillides A.A. Sciatic neurectomy-related cortical bone loss exhibits delayed onset yet stabilises more rapidly than trabecular bone. *Bone Rep.* 2021;15:101116. doi: 10.1016/j.bonr.2021.101116.
- Ko H.Y., Chang J.H., Shin Y.B., Shin M.J., Shin Y.I., Lee C.H. et al. Changes of lower-limb trabecular bone density after sciatic nerve transection in immature rats. *Biomed Res.* 2017;28(18):8079-8084.
- Shimada N., Sakata A., Igarashi T., Takeuchi M., Nishimura S. M1 macrophage infiltration exacerbate muscle/bone atrophy after peripheral nerve injury. *BMC Musculoskelet Disord.* 2020;21(1):44. doi: 10.1186/s12891-020-3069-z.
- Piet J., Hu D., Baron R., Shefelbine S.J. Bone adaptation compensates resorption when sciatic neurectomy is followed by low magnitude induced loading. *Bone.* 2019;120:487-494. doi: 10.1016/j.bone.2018.12.017.
- Tamaki H., Yotani K., Ogita F., Hayao K., Kirimto H., Onishi H. et al. Low-Frequency Electrical Stimulation of Denervated Skeletal Muscle Retards Muscle and Trabecular Bone Loss in Aged Rats. *Int J Med Sci.* 2019;16(6):822-830. doi: 10.7150/ijms.32590.
- Ma X., Lv J., Sun X., Ma J., Xing G., Wang Y. et al. Naringin ameliorates bone loss induced by sciatic neurectomy and increases Semaphorin 3A expression in denervated bone. *Sci Rep.* 2016;6:24562. doi: 10.1038/srep24562.
- Shchudlo N.A., Kobyzhev A.E., Varsegova T.N., Stupina T.A. Histomorphometric assessment of the tibial nerve and small muscles of the foot after internal neurolysis and autogenous plastic surgery of the tibial portion of the sciatic nerve in rats. *Orthopaedic Genius.* 2022;28(6):823-829. (In Russian). doi: 10.18019/1028-4427-2022-28-6-823-829.
- Shchudlo M.M., Stupina T.A., Shchudlo N.A. Quantitative analysis of articular cartilage metachromasia in telepathology. *Proceedings of the Chelyabinsk Scientific Center of the Ural Branch of the Russian Academy of Sciences.* 2004;25:17-22. (In Russian).

24. Scholz T., Krichevsky A., Sumarto A., Jaffurs D., Wirth G.A., Paydar K. et al. Peripheral nerve injuries: an international survey of current treatments and future perspectives. *J Reconstr Microsurg.* 2009;25(6):339-344. doi: 10.1055/s-0029-1215529.
25. Höke A. A (heat) shock to the system promotes peripheral nerve regeneration. *J Clin Invest.* 2011;121(11):4231-4234. doi: 10.1172/JCI59320.
26. Scheib J., Höke A. Advances in peripheral nerve regeneration. *Nat Rev Neurol.* 2013;9(12):668-676. doi: 10.1038/nrneurol.2013.227.
27. Grigorovskii V.V., Strafun S.S., Gaiko O.G., Gaiovich V.V., Blinova E.N. Histopathological changes and correlations of the morphological values of limb muscle status and clinical data in patients with the consequences of innervation traumatic disorders. *Orthopaedic Genius.* 2014;(4):49-57. (In Russian).
28. Kambiz S., Duraku L.S., Baas M., Nijhuis T.H., Cosgun S.G., Hovius S.E. et al. Long-term follow-up of peptidergic and nonpeptidergic reinnervation of the epidermis following sciatic nerve reconstruction in rats. *J Neurosurg.* 2015;123(1):254-269. doi: 10.3171/2014.12.JNS141075.
29. Ikeda M., Oka Y. The relationship between nerve conduction velocity and fiber morphology during peripheral nerve regeneration. *Brain Behav.* 2012;2(4):382-390. doi: 10.1002/brb3.61.
30. Şipos R.S., Fechete R., Moldovan D., Sus I. Szasz S., Pávai Z. Assessment of femoral bone osteoporosis in rats treated with simvastatin or fenofibrate. *Open Life Sci.* 2015;10(1):379-387. doi: 10.1515/biol-2015-0039.
31. Zhang C., Yan B., Cui Z., Cui S., Zhang T., Wang X. et al. Bone regeneration in minipigs by intrafibrillarly-mineralized collagen loaded with autologous periodontal ligament stem cells. *Sci Rep.* 2017;7(1):10519. doi: 10.1038/s41598-017-11155-7.
32. Li C.Y., Price C., Delisser K., Nasser P., Laudier D., Clement M. et al. Long-term disuse osteoporosis seems less sensitive to bisphosphonate treatment than other osteoporosis. *J Bone Miner Res.* 2005;20(1):117-124. doi: 10.1359/JBMR.041010.
33. Singh I.J., Gunberg D.L. Quantitative histology of changes with age in rat bone cortex. *J Morphol.* 1971;133(2):241-251. doi: 10.1002/jmor.1051330208.
34. Piemontese M., Almeida M., Robling A.G., Kim H.N., Xiong J., Thostenson J.D. et al. Old age causes de novo intracortical bone remodeling and porosity in mice. *JCI Insight.* 2017;2(17):e93771. doi: 10.1172/jci.insight.93771.
35. Udinceva M.Ju., Zajcev D.V., Volokitina E.A., Antropova I.P., Kutepov S.M. Investigation of bone tissue mechanical properties in the supra-acetabular region. *Orthopaedic Genius.* 2022;28(4):559-564. (In Russian). doi: 10.18019/1028-4427-2022-28-4-559-564.

Authors' information

✉ Tatyana A. Stupina — Dr. Sci. (Biol.)
Address: 6, M. Ulyanova st., Kurgan, 640014, Russia
<https://orcid.org/0000-0003-3434-0372>
e-mail: stupinasta@mail.ru

Nathalia A. Shchudlo — Dr. Sci. (Med.)
<https://orcid.org/0000-0001-9914-8563>
e-mail: nshchudlo@mail.ru

Tatyana N. Varsegova — Dr. Sci. (Biol.)
<https://orcid.org/0000-0001-5430-2045>
e-mail: varstn@mail.ru